# Variations of magnetic properties of $UGa_2$ under pressure

A. V. Kolomiets,[1,2] J.-C. Griveau,[3] J. Prchal,[1] A. V. Andreev,[4] and L. Havela[1]

[1]*Department of Condensed Matter Physics, Faculty of Mathematics and Physics, Charles University in Prague, Ke Karlovu 5, 121 16 Prague 2, Czech Republic*

[2]*Department of Physics, Lviv Polytechnic National University, 12 Bandera Street, 79013 Lviv, Ukraine*

[3]*European Commission, Joint Research Centre, Institute for Transuranium Elements, Postfach 2340, D-76125 Karlsruhe, Germany*

[4]*Institute of Physics ASCR, Na Slovance 2, 18221 Prague 8, Czech Republic*

(Received 17 February 2014; revised manuscript received 11 November 2014; published 3 February 2015)

Electrical resistivity $\rho(T)$ of the $5f$-ferromagnet $UGa_2$ was investigated on single-crystalline samples as a function of pressure and magnetic field. Under quasihydrostatic pressure the Curie temperature monotonously increases from $T_C = 124$ K up to 154 K at $p = 14.2$ GPa after which it turns down steeply and reaches $T_C = 147$ K at $p = 15.2$ GPa. At 20 GPa the compound is already nonmagnetic. This dramatic variation is compatible with the exchange interactions mediated by the $5f$ hybridization with the non-$f$ states. The external pressure first enhances the exchange coupling of the $5f$ moment but eventually suppresses the magnetic order by washing out the $5f$ moments. Such a two-band model is adequate for the weakly delocalized $5f$ states. The external pressure gradually suppresses the spin-disorder resistivity, which reaches very high $\rho$ values (300 $\mu\Omega$ cm) above $T_C$ in $UGa_2$. This leads to the crossover from the initial negative to the positive $d\rho/dT$ in the paramagnetic state.

DOI: 10.1103/PhysRevB.91.064405 PACS number(s): 71.28.+d, 75.30.−m, 71.27.+a

## I. INTRODUCTION

$UGa_2$ crystallizes in the hexagonal $AlB_2$-type crystal structure (space group $P6/mmm$, $a = 4.213$ Å and $c = 4.012$ Å) [1] first reported in Ref. [2] and later confirmed by numerous authors. The lattice undergoes orthorhombic distortion in conjunction with magnetic ordering [1]. The reduction in symmetry may also influence (as suggested in Ref. [3]) the temperature dependence of the electrical resistivity. The application of external pressure of about 16 GPa leads allegedly to the reversible structural transformation to the tetragonal structure of the $Cu_2Sb$ type with $a = 4.648(19)$ Å and $c = 6.316(36)$ Å [4]. In the same high-pressure study, the bulk modulus of the $AlB_2$ type was reported to be $B_0 = 100 \pm 7.6$ GPa, which is close to the values found for the $RGa_2$ ($R$ = rare − earth) compounds and is more than 1.5 times lower than that of $ThGa_2$.

$UGa_2$ is a collinear ferromagnet with the Curie temperature $T_C = 125$ K [1] and magnetic moment of uranium $\mu_U = 3.0(2)\mu_B$ determined by a neutron-diffraction study [5], whereas 2.71 $\mu_B$/U was obtained from spontaneous magnetization measurements at $T = 4.2$ K [1]. The Curie-Weiss fits of the susceptibility data above $T_C$ yielded the effective moments $\mu_{eff} = 3.0\mu_B$/U ($\Theta_p = 125$ K) and $\mu_{eff} = 3.55\mu_B$/U ($\Theta_p = -148$ K) for $H \| a$ and $H \| c$, respectively [1]. Both $T_C$ and $\mu_U$ are higher than the typical values found for ferromagnetic uranium intermetallics, although $\mu_U$ is still lower than 3.25 $\mu_B$/U or 3.33 $\mu_B$/U expected for $5f^2(U^{4+})$ or $5f^3(U^{3+})$ configurations in the intermediate coupling scheme. The compound shows pronounced magnetocrystalline anisotropy. The [100] ($a$ axis) is the easy magnetization direction, the magnetization along the [120] direction ($b$ axis) is clearly lower, and [001] ($c$ axis) is the hard direction with an estimated anisotropy field of the range 300 T [1]. The powder neutron diffraction has corroborated the nonmagnetic state of gallium and the in-plane orientation of the uranium magnetic moments. Yet it did not provide any further specifics about the moment orientation [5].

The electronic contribution to the specific heat $\gamma = 10$ mJ mol$^{-1}$K$^{-2}$ [6,7] is comparable to the value reported for $LaGa_2$, $\gamma = 5$ mJ mol$^{-1}$K$^{-2}$ [8] and points to the absence of high density of electronic states at the Fermi level. One reason for this could be naturally the $5f$ localization. Polarized neutron data [9] have possibly indicated the $U^{4+}$ state. The localized $5f$ states were suggested by the *ab initio* band structure [10] and crystalline electric-field (CEF) calculations [11], although there remained uncertainty whether they are of the $5f^2$ or $5f^3$ type. The opposite, i.e., itinerant character of the $5f$ states, was deduced from photoemission studies [12]. Finally, the magnetoresistance and de Haas–van Alphen (dHvA) experiments [6] could not be convincingly explained by either the localized or the itinerant model if calculating the Fermi surface in the local spin-density approximation.

The uncertainty about the character of the $5f$ states was one of the main reasons for the high-pressure studies described in the present paper. The variations of the ordering temperature driven by the lattice compression serves as an indicator of the nature of the electronic states which are involved in the magnetic-moment formation and exchange interactions. Application of external pressure to a band system typically leads to the suppression of the magnetic moments as well as the reduction in the ordering temperature, resulting from a pressure-induced band broadening. Such a negative pressure effect is also connected with the positive magnetovolume relation: The formation of the magnetic moments is accompanied by a relatively large increase in the atomic volume and vice versa [13]. Should the magnetic interactions involve localized states, the external pressure would have little effect on the magnetic moments and their ordering temperatures. In some cases the critical temperature may even weakly increase due to small changes in the Ruderman-Kittel-Kasuya-Yosida (RKKY) interaction [13].

In the exceptional cases pressure can support magnetic-moment formation. For instance in Yb, it promotes the smaller magnetic $4f^{13}$ state on account of the larger nonmagnetic

 

$4f^{14}$ state. No such effect is, however, expected for U, which is very far from the nonmagnetic $5f^6$ state. Nevertheless, a significant increase of the Curie temperature in $UGa_2$ under pressure found in magnetization and electrical resistivity was reported earlier [13–15], but it was based on a relatively limited pressure range of $p \leqslant 0.8$ GPa. Preliminary data from our present study have suggested that the increase extends over a much larger pressure range, implying that the strengthening of the $5f$-ligand hybridization is the dominant mechanism of the enhancement of exchange interactions [16]. That would classify $UGa_2$ as a material in the interesting regime at the verge of $5f$ localization, which is expected to turn into the standard band ferromagnet only at very high pressures. The $T_C$ value has to go in this case through a maximum. On its high-pressure side the reduction in $T_C$ is expected to be driven by the U-moments washout.

Therefore we may expect that the study of pressure variations of $T_C$ in $UGa_2$ across the whole range of existence of the $AlB_2$ structure and the character of the $5f$ states in $UGa_2$ can be revealed, which should provide guidance for a possible theoretical description.

## II. EXPERIMENTAL DETAILS

The measurements were performed on $UGa_2$ single crystals grown by the Czochralski technique. Laue diffraction (a Micrometa commercial diffractometer) was used for the quality assessment of the crystals as well as their orientation. A twinning with approximately 2° misalignment of the $a$ axis between the grains was found. Resistivity measurements at ambient pressure were carried out by the four-probe method in the Quantum Design physical property measurement system (PPMS) equipped with a 14-T magnet in the temperature range from 2 to 300 K. The sample size varied from 0.5 to 2 $mm^3$. The Quantum Design Magnetic Property Measurement System and Physical Property Measurement System were used for the magnetization measurements in the temperature range from 2 to 650 K. The measurements were performed in the extraction and vibrating-sample magnetometer modes.

High-pressure resistivity measurements were performed by the four-probe dc method in a Bridgman-type clamped pressure cell with the solid pressure-transmitting medium (steatite), using the thin stripe of Pb as a manometer. Before each measurement the cell was loaded and clamped at room temperature. The exact pressure value inside the pressure cell was determined later by following the critical temperature of the superconducting transition of Pb [17]. The error bars of the pressure determination are due to the finite width of the superconducting transition of Pb, which is typically 5%–10% of the absolute value of $T_c$ in the present experiment that yields a typical precision of 0.2 GPa.

Due to a possible change in the sample shape as well as the contacts position during pressurization, the absolute values of the resistivity could be calculated only with substantial uncertainty. Therefore, the resistivities measured at high pressures are presented in arbitrary units. Two different sets of samples were used in these experiments providing independent mutually consistent results.

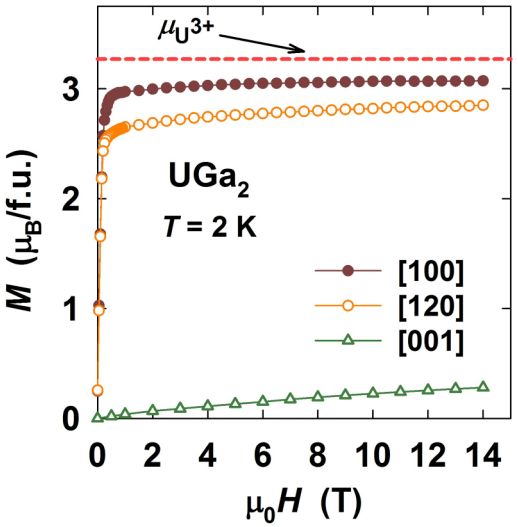


FIG. 1. (Color online) Field dependence of the magnetization of $UGa_2$ measured at $T = 4.2$ K for different crystallographic directions. The dashed line indicates the magnetic moment of $U^{3+}$.

## III. RESULTS

The quality of as-synthesized single crystals as well as their orientation was verified by the magnetization measurements on one of the pieces from the original ingot. The temperature dependence of the magnetization has the typical shape for the ferromagnet with a steep drop at the Curie temperature. The $T_C$ value of 124 K determined from the measurement in the field of 0.1 T is in good agreement with previous literature data. The field dependence of the magnetization (Fig. 1) is also typical for the easy-plane ferromagnet with ⟨100⟩ as the easy axis ($a$ axis). The sample used in this study has reached the saturation value of $M_{sat} = 3.07\ \mu_B$/f.u. (where f.u. represents formula units). The magnetization for the $b$ axis reaches 2.85 $\mu_B$/f.u. at 14 T but is still far from saturation. The hard-axis magnetization ($c$ axis) is more than ten times lower in $\mu_0 H = 14$ T compared to the easy-axis one. The temperature dependence of magnetization measured up to $T = 650$ K in the $H \parallel c$ configuration has the effective moment close to the value given in Ref. [1].

The good quality of the single crystal is indicated by the high ratio $R_{300\,K}/R_{2\,K} = 120$. Temperature scans $\rho(T)$ performed in the zero field for the two current orientations $i \parallel a$ and $i \parallel c$ are shown in Fig. 2. The overall shape and the absolute values of the resistivity are here in good agreement with the literature data [3]. The striking features of the $UGa_2$ resistivity are its very high absolute value in the paramagnetic state, exceeding the common Mott limit of metallic resistivity of 200 $\mu\Omega$ cm [18] (especially for $i \parallel c$), and the negative resistivity slope $d\rho(T)dT < 0$ above the ordering temperature. Several scenarios can lead to such resistivity shapes, and the most typical among them will be discussed below.

First, the Mott (or Mott-Ioffe-Regel) limit itself expresses the fact that the mean-free path of conduction electrons cannot be shorter than the interatomic spacing. For ordinary metals with several conduction electrons per atom and regular spacing of atoms it gives an approximate limit of the maximum metallic resistivity in the range between 100 and 200 $\mu\Omega$ cm.

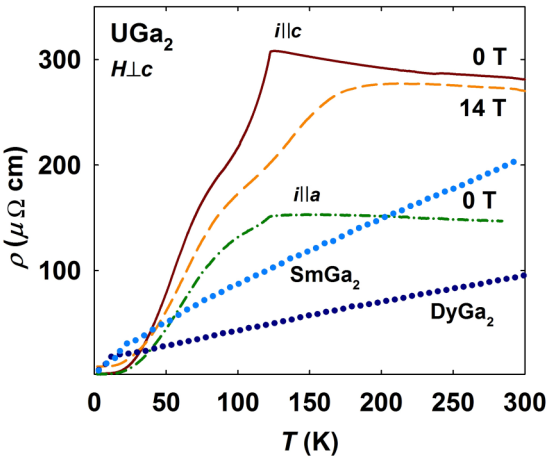


FIG. 2. (Color online) Resistivity of $UGa_2$ for the current $i \parallel a$ (0 T) and $i \parallel c$ (0 and 14 T). Magnetic field $H$ was applied perpendicularly to the $c$ axis. Vertical markers indicate the Curie temperature. The resistivity curves (dotted lines) of $DyGa_2$ and $SmGa_2$ polycrystals from Ref. [17] are included for comparison.

It implies that individual contributions to resistivity are not additive anymore as the limit is approached, i.e., the Matthiessen's rule of additivity cannot be applied to separate individual contributions. As shown by Mooij [19], increasing the resistivity in disordered alloys up to the Mott limit leads to a weak negative slope $d\rho(T)dT < 0$. Although such an effect was originally attributed to special features of the density of states $N(E_F)$ close to the Fermi level, its general occurrence points rather to weak localization, i.e., a quantum interference effect for an electron wavelength similar to the spacing of scattering centers, which is gradually disrupted by thermal fluctuations [20,21].

Second, the resistivity curves similar to that of $UGa_2$ have been observed even in actinide alloys, e.g., in simple band systems with low U-U spacing as U-Mo alloys [22], which obey the Mott limit restrictions. On the other hand, the resistivity of the whole class of compounds with larger U-U spacing, which can be vaguely classified as narrow-band systems, exceeds the Mott limit considerably. Such systems have often very low residual resistivity (merely $2\,\mu\Omega\,$cm here) pointing to a weak impurity scattering. If the high-resistivity scattering, sometimes accompanied by a negative slope [23,24], appears at high temperatures in the narrow-band systems, it must be related to the spin-disorder scattering in the paramagnetic state or to scattering on spin fluctuations in materials, which do not order at all. In such a case the negative slope can be also due to the thermal disruption of weak localization, but we do not have any direct evidence.

Another well-known scenario, which yields the negative $d\rho/dT$ in, e.g., Ce compounds [25], is the Kondo effect. Yet it should be refused for the cases with a strongly ferromagnetic ground state and low Sommerfeld coefficient $\gamma$ because the Kondo screening yields a strongly correlated nonmagnetic or weakly magnetic state with high $\gamma$. As already mentioned above, the Sommerfeld coefficient of $UGa_2$ is rather low $\gamma = 10\,\mathrm{mJ\,mol^{-1}\,K^{-2}}$ [6,7], suggesting that the Kondo-like scenario is not applicable for this compound.

For completeness, one should consider that the negative $d\rho/dT$ could originate from a specific electron-phonon interaction interfering with the impurity scattering [26]. The fact that the negative slope in the temperature range above $T_C$ is removed by the magnetic field (see Fig. 2) clearly points to the decisive role effect of the spin-disorder scattering and not the electron-phonon scattering. The application of the magnetic field would suppress the fluctuations of the magnetic moments but would hardly affect the phonon spectrum. So at least in the case of $UGa_2$ this scenario can be omitted.

As to the particular features of the resistivity of $UGa_2$, its value at the maximum, which is located just above $T_C$, reaches $300\,\mu\Omega\,$cm. Reference [3] gives an even higher value, namely, $350\,\mu\Omega\,$cm. Such disagreement exceeds somewhat the accuracy of determination of the geometrical factor, which should be better than 10%. However, the difference can be larger for very small samples, the size of which is restricted by the size of the single crystal. The latter is the case of both the present paper and Ref. [3].

Since the Matthiessen's rule is not valid in the case of $UGa_2$, the resistivity of a nonmagnetic analog cannot be simply subtracted to obtain a pure magnetic contribution. The flat $\rho(T)$ curve of $UGa_2$ in the paramagnetic state means that the electron-phonon scattering makes only a relatively small contribution. This is different in the rare-earth analogs $RGa_2$, which are isostructural to $UGa_2$, namely, their resistivity increases monotonously at least until 300 K (Fig. 2).The $RGa_2$ intermetallics are antiferromagnets with magnetic ordering temperatures not exceeding 15 K and dominating RKKY exchange interaction. The $\rho(T)$ curve for $DyGa_2$ is typical for the $RGa_2$ series, and $SmGa_2$ has the highest room-temperature resistivity within the series due to the CEF contribution (Fig. 2) [27,28]. Neither these two curves, nor any other for the isostructural $RGa_2$ resemble the $\rho(T)$ temperature dependence of $UGa_2$. The main difference is that lower spin-disorder scattering in $RGa_2$ allows the manifestation of the electron-phonon scattering, responsible for the high-temperature linear increase in resistivity in these compounds.

The contribution to the resistivity due to the spin-disorder scattering in $RGa_2$ is $40\,\mu\Omega\,$cm or less, despite much higher moments especially for heavy rare earths [29]. This indicates much stronger coupling of the $5f$ moments ($UGa_2$) to conduction electrons comparing with the $4f$ counterparts ($RGa_2$). In general, the ordering temperatures and the spin-disorder scattering contribution are ten times higher in $UGa_2$ compared to $RGa_2$ analogs. On the other hand, in the same compounds the magnetic moments of uranium atoms are about three times lower than those of the heavy rare earths. It is known that for the RKKY interaction both the ordering temperature and the spin-disorder scattering scale with $(g-1)^2 J(J+1)J_{sf}^2$—the product of the squared magnetic moment and $J_{sf}$, the exchange-coupling strength between the $4f$ and the conduction electrons. Considering this, one arrives at the conclusion that the effective exchange coupling $J_{sf}$ in $UGa_2$ must be about two orders of magnitude higher than, e.g., in $DyGa_2$.

The transition temperature in $UGa_2$ corresponds to the steep drop in electrical resistivity. We have associated $T_C$ with the maximum of $d\rho(T)/dT$, which yields $T_C = 122\,$K for $i \parallel c$. The decrease below $T_C$ is slowed down by a hump seen for both current directions. Reference [6] associates its occurrence

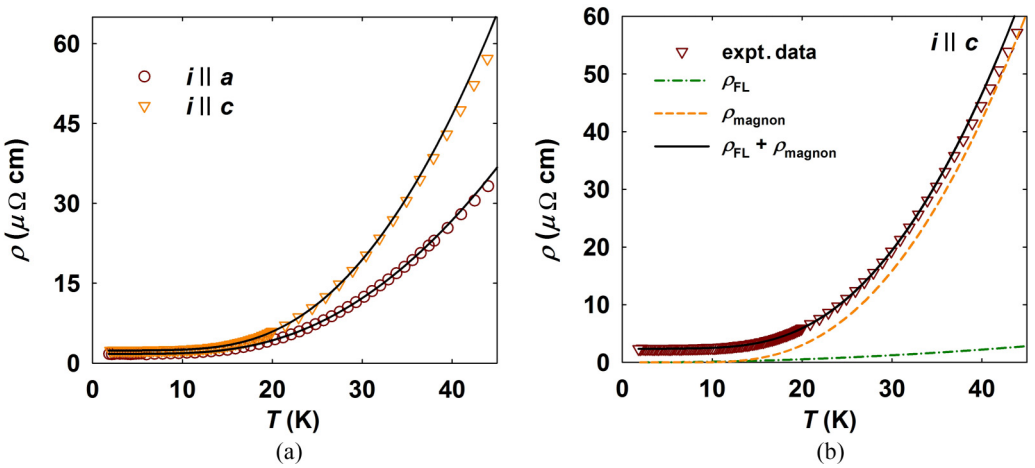


FIG. 3. (Color online) (a) Zero-field low-temperature resistivity of $UGa_2$ for different current configurations. Solid lines represent the fits to Eq. (1). Note: To improve the readability, only one point out of three is plotted. (b) Comparison of the Fermi-liquid ($\rho_{FL}$) and magnon ($\rho_{magnon}$) contributions to the zero-field electrical resistivity of $UGa_2$. Note: To improve the readability, only one point out of three is plotted.

with the lattice distortion, although in our opinion there is no real evidence that the distortion would start not at the critical temperature but 25 K below it. The origin of the hump remains therefore unclear.

The Curie temperature for $i \parallel a$ is located at the same temperature as for $i \parallel c$ and corresponds to the similar drop in $\rho(T)$, although it is much less pronounced in the former case, and even at ambient pressure it is rather difficult to locate. At low temperatures both resistivity curves drop to very low values, and 1.8 and 2.3 $\mu\Omega$ cm are achieved at the minimum temperature $T = 1.8$ K for $i \parallel a$ and $i \parallel c$, respectively.

We can assume that the contribution from the electron-phonon scattering, which follows the $T^3$ dependence in the transition metals with states of higher effective mass present at $E_F$ (compared to simple metals having the $T^5$ low-temperature scaling of the electron-phonon term), may be small at low temperatures. For instance, Ref. [29] indicates that resistivity of nonmagnetic $LaGa_2$ reaches only approximately 10 $\mu\Omega$ cm at $T = 50$ K. Therefore, we have tentatively analyzed the resistivity curves of $UGa_2$ measured below 30 K in both current orientations using the expression,

$$\rho(T) = \rho_0 + AT^2 + BT(1 + 2T/\Delta)\exp(-\Delta/T). \quad (1)$$

The two first terms of this equation represent the Fermi-liquid approximation of the electron-electron scattering. The third term is due to the magnon contribution (electron-magnon scattering), which is assumed to dominate because of the strong spin-disorder scattering. Such expressions should describe $\rho(T)$ well below $T_C$ where magnons as low-energy magnetic excitations dominate and where the resistivity values are far below the Mott limit. The parameter $\Delta$ corresponds to the minimum magnon excitation energy (magnon gap), which is the lowest magnetic anisotropy energy—in $UGa_2$ that would be most likely the anisotropy in the basal plane. The estimate of the in-plane anisotropy from the magnetization data (Fig. 1) by the linear extrapolation of the [120] $M(H)$ dependence until the crossing point with the [100] curve yields the value of 32 T or, considering the 3 $\mu_B$/U magnetic moment, $\Delta$ of approximately 96 K.

As seen from Fig. 3(a), Eq. (1) is suitable for the description of the resistivity curves for both current directions $i \parallel a$ and $i \parallel c$. The fitting parameters for the temperature range of 1.8 K $< T <$ 30 K are shown in Table I. They point to the larger contribution of the magnon term for the $i \parallel c$ configuration compared to $i \parallel a$, which is in agreement with the generally stronger spin-disorder scattering. The spin gap of about 60 K is in reasonable agreement with the 96-K estimate for the in-plane anisotropy. The Fermi-liquid coefficient $A$ corresponds to the value expected on the basis of the Kadowaki-Woods relation $A/\gamma^2 = 10^{-5}(\mu\Omega\,\text{cm K}^{-2})(\text{mJ mol}^{-1}\,\text{K}^{-2})^2$, which yields $A = 1 \times 10^{-3}\,\mu\Omega\,\text{cm K}^{-2}$ for $\gamma = 10\,\text{mJ mol}^{-1}\,\text{K}^{-2}$. Notably, Fig. 3(b) reveals that the Fermi-liquid contribution represents actually only a very small fraction of the total resistivity.

The contributions of the electron-electron ($\rho_{FL}$) and the electron-magnon ($\rho_{magnon}$) scatterings to the electrical resistivity of $UGa_2$ are illustrated in Fig. 3(b) using the zero-field $i \parallel c$ measurement as the example. It shows that the magnon contribution dominates at temperatures below 35 K, above which Eq. (1) becomes no longer adequate for the description of the experimental data.

The application of the magnetic field perpendicular to the $c$ axis affects the $\rho(T)$ dependence in the whole temperature range (Fig. 2): it increases the resistivity at the low-temperature end whereas the effect at high temperatures is opposite. The crossing point between these two regions for the field of 14 T is around 36 K. The most pronounced change

TABLE I. The fitting parameters for Eq. (1) applied to the zero-field resistivity of $UGa_2$.

| | $\rho_0$ ($\mu\Omega$ cm) | $A$ ($\mu\Omega\,\text{cm K}^{-2}$) | $B$ ($\mu\Omega\,\text{cm K}^{-1}$) | $\Delta$ (K) |
|---|---|---|---|---|
| | | 0 T | | |
| $i \parallel a$ | 1.7 | $1.1 \times 10^{-3}$ | 0.9 | 54 |
| $i \parallel c$ | 2.4 | $1.4 \times 10^{-3}$ | 2.4 | 65 |
| | | 14 T ($H \perp c$) | | |
| $i \parallel c$ | 9.0 | $2.0 \times 10^{-3}$ | 2.4 | 63 |

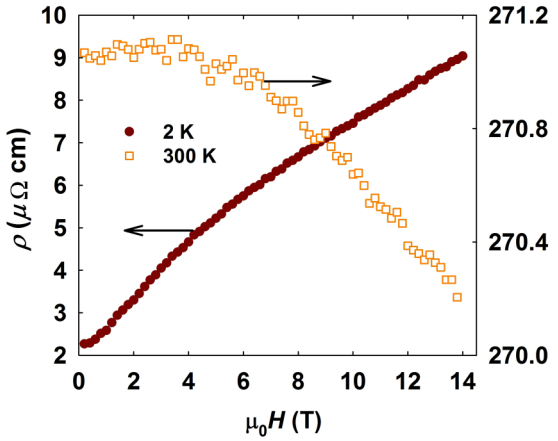


FIG. 4. (Color online) Field variation of the resistivities measured at $T = 2\,\mathrm{K}$ (full circles) and 300 K (open circles) for $UGa_2$ in the $i \parallel c$ configuration. Note two vertical axes.

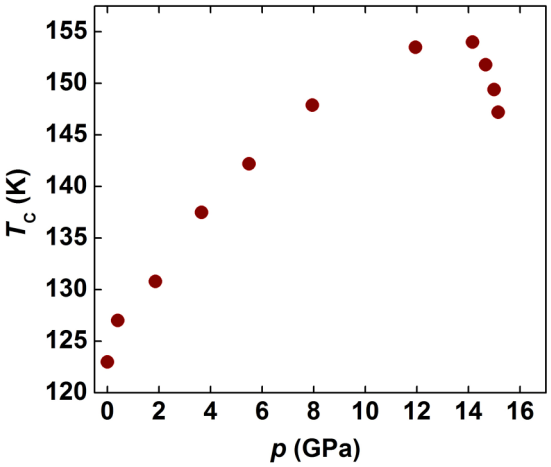


FIG. 6. (Color online) Pressure dependence of the Curie temperature of $UGa_2$.

in the resistivity dependence takes place in the vicinity of the Curie temperature, where the $T_C$ anomaly shifts from 122 K (0 T) to 136 K (14 T). The field-induced shift and broadening of the anomaly towards higher temperatures is common in ferromagnets. The negative $d\rho/dT$ is almost entirely removed by the magnetic field, and the resistivity at $T_C$ drops by a factor of 1/3, i.e., by approximately $100\,\mu\Omega\,\mathrm{cm}$, compared to its value at $H = 0$ (see Fig. 2). The changes in the residual resistivity, which increases more than three times from 2 to $9\,\mu\Omega\,\mathrm{cm}$ (Fig. 4), can be attributed to the normal magnetoresistance. The room-temperature resistivity is affected less by the field increase: It remains nearly constant until 6 T and then continuously decreases by 9% as 14 T is reached. Equation (1) is still suitable for the description of the 14-T data, and it yields $\Delta = 63\,\mathrm{K}$, $\rho_0 = 9.0\,\mu\Omega\,\mathrm{cm}$, $A = 2.0 \times 10^{-3}\,\mu\Omega\,\mathrm{cm\,K^{-2}}$. The coefficient $B$ remains unchanged within the precision of the fit. The temperature range, across which Eq. (1) can be applied, shrinks from $2\,\mathrm{K} < T < 30\,\mathrm{K}$ in the zero field to $2\,\mathrm{K} < T < 18\,\mathrm{K}$ in 14 T.

High-pressure resistivity measurements were performed using only the $i \parallel c$ current orientation because the anomaly at the Curie temperature is more pronounced compared to the $i \parallel a$ setup. Hence, the $i \parallel c$ setup provides a more reliable estimate of the $T_C$ for the compressed sample, despite that the $\rho(T)$ features are broadened, perhaps due to a nonhydrostaticity.

As seen from Fig. 5(a), the $\rho(T)$ shape gradually evolves with increasing pressure with no sudden jumps or discontinuities. One can clearly recognize that the Curie temperature increases with increasing pressure. This change is well illustrated by the blowup of the transition region [Fig. 5(b)]. The drop in the resistivity associated with the transition is shifted towards higher temperatures with increasing pressure. The analysis of the first derivative for each $\rho(T)$ dependence was used to establish the precise values of $T_C$ at all pressures (Fig. 6). It was found that the Curie temperature of $UGa_2$ increases

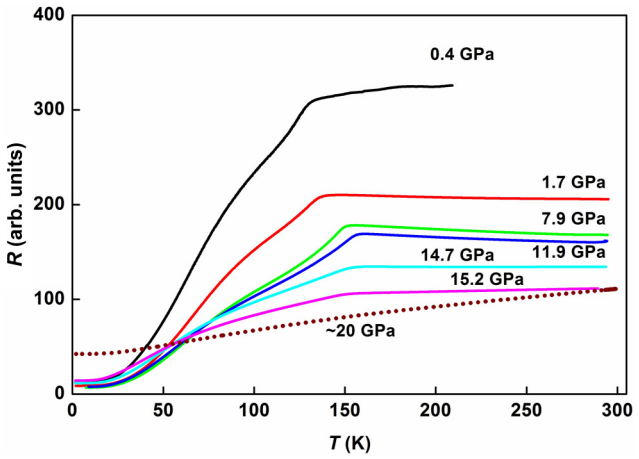


(a)

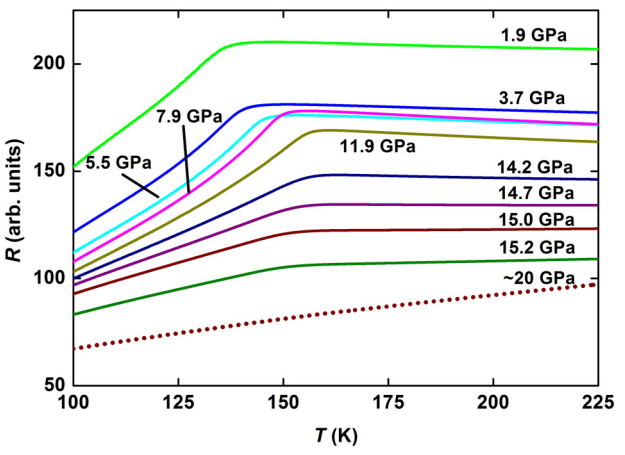


(b)

FIG. 5. (Color online) (a) Selected resistivity curves measured of $UGa_2$ measured in the $i \parallel c$ configuration. The dotted line represents the data collected on the sample, which has been exposed to the pressure over 16 GPa. (b) Details of the resistivity curves of $UGa_2$ in the transition region ($i \parallel c$ configuration). The dotted line represents the data collected on the sample, which has been exposed to the pressure over 16 GPa.

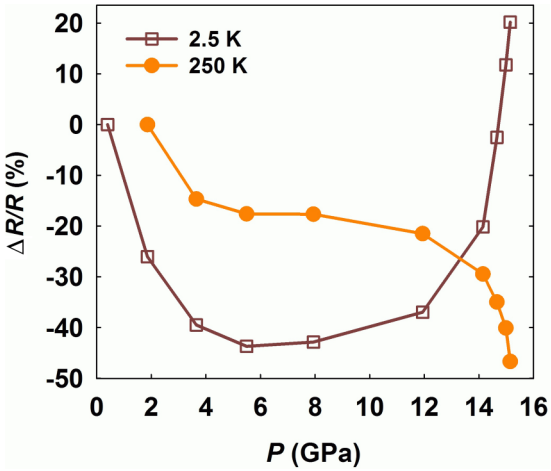


FIG. 7. (Color online) Pressure effect on the resistivity of $UGa_2$ at $T = 2.5$ K (open squares) and 250 K (full circles). The resistivities were compared with the respective values at $p = 0.4$ GPa. The lines are guides to the eye.

with increasing pressure until $T_C = 154$ K at $p = 14.2$ GPa. Above this pressure the Curie temperature starts to decrease much steeper than it has been increasing. The closer inspection of the $T_C(p)$ dependence suggests that the maximal value of $T_C$ is reached at about $p = 13$ GPa although there are no experimental data at this pressure value. At $p = 15.2$ GPa, $UGa_2$ is still ferromagnetic with the ordering temperature $T_C = 147$ K.

One of the samples was loaded to the pressure between 19.5 and 21 GPa [dotted lines in Figs. 5(a) and 5(b)]. In such a state it did not show any traces of the magnetic phase transition. Enhanced $\rho_0$ in such a state could be due to the structural transformation, which was reported around 16 GPa [6]. Since the contacts to the sample were not lost and its $\rho_{300\,K}$ value corresponded to the value expected from the $\rho_{300\,K}(p)$ dependence for the other pressures (Fig. 7), we assume that the suppression of the magnetic order in $UGa_2$ indeed takes place between 15.2 and 21 GPa. Due to the lack of the experimental data in this pressure range the exact value of the critical pressure could not be determined. Still it should be mentioned that the extrapolation of the $T_C(p)$ dependence (Fig. 6) to the intercept with the temperature axis suggests that $T_C$ should turn to zero between 16 and 18 GPa. As for the high-pressure structure, Ref. [4] indicated the possibility of continuous modifications of interplanar distances. However, a clear identification of the high-pressure structure is necessary in order to establish the correlation between the structure and the magnetism of the high-pressure phase.

When analyzing $\rho(T)$ obtained in the high-pressure experiment, one should consider the variation of the geometrical factor during the pressure increase, which makes the absolute resistivity values unreliable. Since the contacts are not firmly attached to the sample in this type of cell, we particularly expect small variations in the region 1-2 GPa, whereas at higher pressures the contacts are typically already immobilized. We assume that this is the most plausible reason for the resistivity drop between 0.4 and 1.7 GPa [Fig. 5(a)]. By comparing the data collected above 1.7 GPa [Figs. 5(a) and 5(b)] we indeed observed a smooth (if any) variation of the geometrical factor in our experiment, and therefore, we consider the pressure-induced changes in the residual and room-temperature resistivities to be intrinsic. Although the contacts can in principle still shift in this pressure range, a typical fingerprint is a large sudden change, which is absent here.

The residual resistivity, which could be reasonably well represented by the $\rho(2.5\,K)$ value, has the U-shaped pressure dependence with a minimum between 6 and 8 GPa with a progressive increase in the high-pressure side (Fig. 7). Contrary to $\rho(2.5\,K)$, the room-temperature resistivity is reduced under pressure (Fig. 7). Since the $\rho(T)$ curves in the pressure cell could be reliably measured only until approximately $T = 250$ K, the value $\rho(250\,K)$ is used as an indicator instead of $\rho(300\,K)$. As seen from Fig. 7, $\rho(250\,K)$ decreases in the whole pressure range. It develops through a plateau between 3 and 8 GPa after which turns downwards and drops steeply above 12 GPa. The similarity of the pressure values, at which both $\rho(2.5\,K)$ and $\rho(250\,K)$ change their characters, suggests that the phenomena behind their pressure variations may be the same.

The steep variation of both residual and room-temperature resistivities is not the only qualitative change which takes place around 12 GPa. The character of the whole $\rho(T)$ dependence changes in the same pressure range (Fig. 8). The anomalous decrease in the resistivity with increasing $T$ in the paramagnetic state was found for all pressures below $p = 12.5$ GPa. At $p = 14.7$ GPa a local minimum appears at $T \approx 220$ K. Finally, $d\rho/dT > 0$ at $p = 15.0$ GPa.

The low-temperature resistivity of $UGa_2$ can be fitted to Eq. (1) for all pressures. The temperature range in which the fit is valid shrinks somewhat with increasing pressure: Its upper limit shifts from 35 K at ambient pressure to 20 K at 15 GPa. Still the agreement between the experimental data and the fit remains quite good. The obtained fitting parameters are shown in Fig. 9. The character of their pressure dependence points to the increase in the magnon band gap. The energy of the magnon band gap is a measure of magnetic anisotropy energy per one U atom; it may be understood as due to strengthening of hybridization, which is an important ingredient of the two-ion anisotropy. Its decrease in the high-pressure range can be related to the suppression of U magnetic moments.

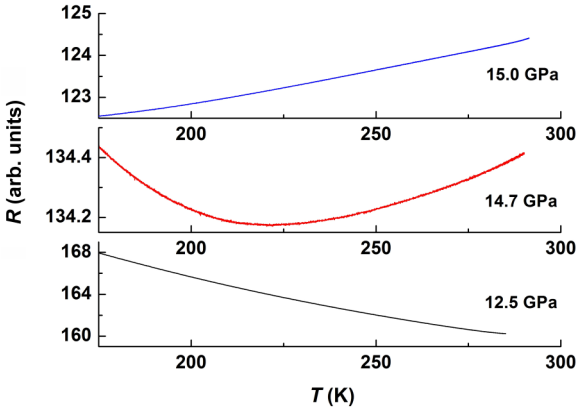


FIG. 8. (Color online) Positive $d\rho/dT$ in the paramagnetic state developing with pressure.

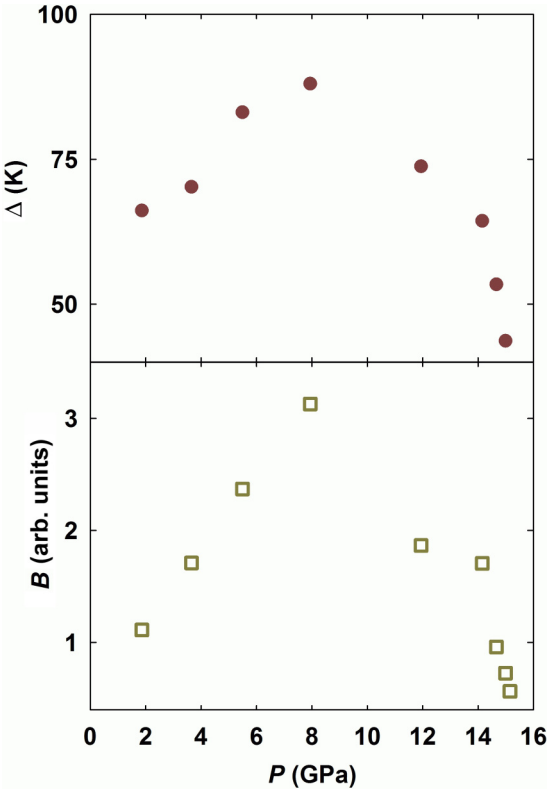


FIG. 9. (Color online) Pressure variation of the magnon band gap and the prefactor $B$ of the magnon term in Eq. (1).

The prefactor $B$ develops very similarly. It contains, besides parameters of the Fermi level, the strength of coupling of the conduction electrons to the spins of $5f$ states, which is also likely supported by pressure, until the $5f$ moments plunge. The prefactor $A$ of the Fermi-liquid term exhibits a weakly increasing tendency, which can attest to the increasing density of states at $E_F$, also corresponding to the stronger hybridization of the conduction-electron states at the Fermi level with the $5f$ states, which practically do not contribute to $N(E_F)$ at ambient pressure. The uncertainty is, however, high due to the relatively small contribution of the $e$-$e$ scattering to the total resistivity.

## IV. DISCUSSION

The obtained experimental results indicate that the $5f$ states of uranium in $UGa_2$ are not the common band states. In such a case the ordering temperature would decrease with pressure from the beginning. Neither are they fully localized since that would presume very small changes in $T_C$. An intermediate situation is the only scenario consistent with the observed pressure variation of the critical temperature, namely, its pronounced increase followed by the saturation and the subsequent drop.

Such nonmonotonous behavior can be obtained, for example, in the framework of the Doniach necklace model [30]. In this model, both the RKKY interaction and the Kondo interaction depend on the exchange parameter $J$ between local spins and spins of conduction electrons. Strengthening of the hybridization leads to an increase in $J$, which first increases the intersite exchange coupling, but when it becomes too strong, the Kondo screening leads to the collapse of the local moments and magnetic order vanishes. Such a model is often used for, e.g., Ce-based materials. It is, however, not quantitatively applicable to the strongly ferromagnetic U compounds. We would have to assume that the exchange interaction is of the simple RKKY type. As discussed above, it is not the case because the ordering temperature of $UGa_2$ is an order of magnitude higher than that of $RGa_2$ compounds with the RKKY interaction, although the latter ones have much higher spin moments. Even more importantly, in such a case we would have to assume that the Kondo effect is the mechanism responsible for the suppression of magnetism. The Kondo effect (which can give rise to a negative $d\rho/dT$) is a specific mechanism in which the spin screening or compensation and not the delocalization dominates. We do not have any evidence of spin compensation at $UGa_2$ with U moments of $3\,\mu_B$. At elevated pressures where the Kondo effect could be stronger, we observe, on the other hand, the regular positive slope of resistivity.

The model, which was so far successfully applied to light actinides, is based on hybridization-induced exchange interaction (operating independently on the RKKY mechanism), and it is strongly directional. It is also based on the mixing of the two types of states, namely, strongly correlated $f$ states and conduction-electron states, conceiving their mixing in the terms of the resonant scattering. It extends the Coqblin-Schrieffer theory [31] and provides strongly anisotropic exchange interaction with strong ferromagnetic exchange along the shortest links between the $f$ atoms and the magnetic moments oriented perpendicular to them. The magnetic anisotropy energies in such a case can be very high [32]. In such a model the strengthening of the hybridization due to the reduction in the interatomic spacing by pressure at first leads to stronger effective intersite $5f$-$5f$ exchange interactions. But at a certain stage the hybridization starts to affect the $5f$ moments, which are washed out, and finally the magnetic moments and their ordering are lost in a strongly nonlinear way.

The character of the $T_C(p)$ dependence in $UGa_2$ goes in line with the predictions of such a two-band approach in which the hybridization plays a dual role: On one hand it strengthens the $5f$-$5f$ or $5f$-ligand hybridization, and on the other hand it leads to the washout of the $5f$ magnetic moment due to broadening of the $5f$ states. The maximum of $T_C$ can be interpreted just as the point in which the product of the exchange strength and the squared magnetic moment reach their maximum values. Upon further increase in pressure the strengthening of the exchange interactions is overcompensated by the moments washout. It would be interesting to follow the development of magnetization, but pressures around 10 GPa are currently out of the reach of common techniques yielding quantitative magnetization data. So far, such a pressure-induced increase in the critical temperature has been reported only for a few U compounds, namely, for UTe and USe [33], UPtAl [34], or $UIn_3$ [35]. This makes the case of $UGa_2$ even more interesting. It is, therefore, understandable that standard computational schemes do not give an adequate description of the Fermi-surface topology. It would be interesting to see if the LDA+U (LDA = local-density approximation) methods,

better capturing more localized systems, would explain the experimental observables in dHvA.

The important role of the $5f$-ligand hybridization in mediating the exchange interaction is evident from the fact that the shortest U-U spacing $d_{U-U} = 4.012$ Å by far exceeds the Hill limit, preventing a direct $5f$-$5f$ overlap. Even after the 11% volume reduction [4] following the application of quasihydrostatic pressure of 15 GPa the $d_{U-U}$ remains in the range of 3.85–3.90 Å, i.e., far above the Hill limit. Here we have assumed the isotropic volume reduction since the individual compressibilities, which could be anisotropic, have not been reported.

It should be pointed out that the situation, in which the $5f$ magnetic moments are forced by anisotropy into the direction perpendicular to the shortest U-U links, is typical for anisotropic hybridization-mediated exchange interaction [32], although it may have a broader validity in those materials where the $5f$ states are involved in anisotropic bonding and strong spin-orbit interaction leads to large orbital moments even in the case of band states [36]. For $UGa_2$ the shorter U-U spacing along the $c$ axis (4.012 Å) compared with the longer one within the basal plane (4.21 Å) implies that the uranium moments are in the plane and a strong ferromagnetic coupling is along $c$. Certain insight is provided by inelastic neutron-diffraction data [37]. They indicate the absence of the crystal-field excitations but show the magnon excitations with dispersion along $c$, confirming that the exchange along $c$ is the prominent driving force of the magnetic ordering. The magnon gap of 7 to 8 meV (80–90 K) is in reasonable agreement with the gap obtained from $\rho(T)$ and with the moderate $a$-$b$ anisotropy, which allows low-energy propagating magnon modes with the U moments perpendicular to $c$. The observation of magnons can serve as additional proof of certain $5f$ localization as band $5f$ systems do not exhibit clear magnon excitations [38].

The dominating role of the $5f$-ligand hybridization can be deduced also from the paper of da Silva *et al.* [8], who have shown that the substitution of Si or Ge for Ga has a more pronounced effect on the Curie temperature of $UGa_2$ than the volume change of the same magnitude but without the modification of the electronic character of the ligand.

Finally, the observation of the uranium moments slightly below the $U^{3+}$ or $U^{4+}$ values and the simultaneous absence of any substantial $5f$ density at the Fermi level as indicated by the low electronic contribution to the specific heat $\gamma = 10\,\mathrm{mJ\,mol^{-1}\,K^{-2}}$ [6,7] also favors the $5f$-ligand hybridization over the pure $5f$-band formation when we consider the main delocalization mechanism of the $5f$ states.

The character of $UGa_2$ in the high-pressure phase existing over 16 GPa remains still unclear as the structure has not been yet identified unambiguously. Although it was mentioned that the symmetry changes from the hexagonal to the tetragonal [4], while the interplanar distances vary continuously across the transition, there are certain doubts as to the structure details of the high-pressure phase. First, the suggested $Cu_2Sb$-type structure is not among the $AlB_2$-type derivatives [39]. Second, the lattice parameters for the high-pressure $Cu_2Sb$-type phase reported in the original paper [4] give higher volumes per 1 f.u. of $UGa_2$ than the ambient pressure $AlB_2$-type hexagonal phase. In our opinion, that calls for further investigation of the structural transition and its role in the suppression of magnetism in $UGa_2$.

The reported results indicate a special position of $UGa_2$ among U compounds. A proximity to the localization of $5f$ electronic states is evidenced by the fact that the simple $5f$-band picture is not compatible with the increase in $T_C$ under pressure. In such a situation it is understandable that the conventional density functional theory calculations cannot explain the Fermi-surface geometry, which affects the dHvA data [3]. It is a matter of fact that the majority of U intermetallics exhibit the $5f$-band states at the Fermi level. The only known exception, at least among binary compounds, is $UPd_3$, where the localized $5f$ states displaced from the Fermi level were clearly identified by photoelectron spectroscopy. There are several other compounds with low-$\gamma$ values, e.g., UPdSn with $\gamma = 5\,\mathrm{mJ\,mol^{-1}\,K^2}$ [40]. However, both dilution studies [41] and spectroscopy data [42,43] speak against the localization. Calculations in this case succeeded to capture the density of states if performed for the real noncollinear magnetic structure [44]. A pressure dependence of the ordering temperature is positive in the case of UPdSn, but the increase is slower than in $UGa_2$ (1.4 K/GPa) and the studied pressure range is limited so the maximum value of $T_N$ is unknown [45]. Also the bulk modulus is unknown, and the variation of $T_N$ cannot be therefore related to the absolute lattice compression parameters.

Another interesting case, helping to determine the location of $UGa_2$ on the landscape of U intermetallics, is $UIn_3$, mentioned above. It is the local moment antiferromagnet with $T_N = 88$ K, which increases up to 127 K for $p = 9$ GPa (i.e., 3 K/GPa). Higher pressures could not be reached [35]. This can be compared with the isostructural $UGa_3$, a $5f$-band antiferromagnet with $T_N = 67$ K, the ordering of which is suppressed by the pressure of 2.5 GPa [46]. When the size of the ligand, which strengthens the $5f$-ligand hybridization, is reduced even more in $UAl_3$, the magnetic ground state is suppressed even at ambient pressure, and $UAl_3$ is a weakly temperature-dependent paramagnet [47]. Unfortunately only basic data are known in the opposite case $UTl_3$ where the hybridization should be the weakest from the series. U moments are larger ($1.6\,\mu_B$) than in $UIn_3$ ($1.0\,\mu_B$) (Ref. [48] and references therein) although the ordering temperatures are comparable. Variations of $T_N$ with pressure are not known.

Considering such facts, we may speculate that the strong increase in ordering temperatures up to a maximum and subsequent downturn may represent a generic type of behavior for compounds of uranium (and perhaps other light actinides), but more systematic evidence is necessary. In none of the high-pressure papers cited above (except for Ref. [33]) the pressure range used did not allow observing any saturation of ordering temperatures. It will be important to compare with other U compounds when relevant data will be available. Even more importantly, the knowledge of pressure variations of the size of moments is essential as the discussion above assumes the collapse of U moments causing the $T_C$ downturn in the high-pressure range. Precise magnetization measurements on single crystals in the range above 10 GPa would be very difficult. Instead, we propose to study pressure variations of U moments by means of x-ray magnetic circular dichroism, which is becoming feasible.

## V. CONCLUSIONS

Studies of the high-quality single crystal of $UGa_2$ have shown that the ferromagnetic ordering temperature of this compound increases with the increasing pressure up to $p \approx 13$ to 14 GPa reaching $T_C = 154$ K after which it decreases rapidly until at least $p = 15.2$ GPa where $T_C = 147$ K. The increase in pressure up to approximately 20 GPa completely suppresses the magnetic ordering. At such pressures another structure type is, however, adopted. Such $T_C(p)$ dependence indicates that the two-band model is applicable for the description of the character of the $5f$ states in $UGa_2$.

The low-temperature resistivity of $UGa_2$ is dominated by the electron-magnon scattering with the excitation energy exceeding 60 K, which is comparable to the magnetocrystalline anisotropy in the $ab$ plane. The magnon gap increases with the increasing pressure reaching the value of $\Delta = 88$ K at $p = 8$ GPa. The resistivity value of $\approx 300\ \mu\Omega$ cm for the $i \parallel c$ geometry in the paramagnetic state can be attributed to a strong spin-disorder scattering, which also leads to a weak negative slope $d\rho/dT < 0$. The high resistivity and its negative slope are removed by pressure, assumed to reduce U magnetic moments. This corroborates the fact that the negative slope is due to strong disorder (originating in spin disorder in this case) and not due to, e.g., the Kondo effect.

The pressure dependences of the magnon gap of the residual and room-temperature resistivities suggest that the pronounced washout of the magnetic moment of uranium in $UGa_2$ starts at about 8 GPa. Within the two-band model scenario and the hybridization-induced exchange, the increase in the hybridization strength above 13 to 14 GPa cannot compensate for the decrease in the magnetic moment anymore, and the magnetic exchange strength reflected in $T_C(p)$ starts to decrease.

## ACKNOWLEDGMENTS

This work was supported by the Czech Science Foundation under Grants No. P204/10/0330 and No. P204/12/0150. The work at ITU Karlsruhe has been supported by the EU funding scheme ACTINET-I3. Experiments at Charles University were performed at MLTL (http://mltl.eu/), which is supported within the program of Czech Research Infrastructures (Project No. LM2011025).

[1] A. Andreev, V. K. Belov, A. Deriagin, V. Z. A. Kazei, R. Z. Levitin, A. Menovsky, Y. F. Popov, and V. I. Silant'ev, Sov. Phys. JETP **48**, 1187 (1978).
[2] E. S. Makarov and V. A. Ledvik, Sov. Phys. Crystallogr. **1**, 506 (1956).
[3] T. Honma *et al.*, Physica B **281-282**, 195 (2000).
[4] N. R. Sanjay Kumar, N. Subramanian, N. V. Chandra Shekar, M. Sekar, and P. C. Sahu, Philos. Mag. Lett. **84**, 791 (2004).
[5] A. C. Lawson, A. Williams, J. L. Smith, P. A. Seeger, J. A. Goldstone, J. A. O'Rourke, and Z. Fisk, J. Magn. Magn. Mater. **50**, 83 (1985).
[6] T. Honma *et al.*, J. Phys. Soc. Jpn. **69**, 2647 (2000).
[7] L. M. da Silva, F. G. Gandra, A. N. Medina, A. O. dos Santos, and L. P. Cardoso, J. Appl. Phys. **97**, 10A921 (2005).
[8] L. M. da Silva, A. O. dos Santos, A. N. Medina, A. A. Coelho, L. P. Cardoso, and F. G. Gandra, J. Phys.: Condens. Matter **21**, 276001 (2009).
[9] R. Ballou, A.V. Deriagin, F. Givord, R. Lemaire, R. Levitin, and F. Tasset, J. Phys., Colloq. **43**, C7-279 (1982).
[10] M. Divis, M. Richter, H. Eschrig, and L. Steinbeck, Phys. Rev. B **53**, 9658 (1996).
[11] R. J. Radwanski and N. H. Kim-Ngan, J. Magn. Magn. Mater. **140–144**, 1373 (1995).
[12] T. Gouder, L. Havela, M. Divis, J. Rebizant, P. M. Oppeneer, and M. Richter, J. Alloys Compd. **314**, 7 (2001).
[13] J. J. M. Franse, P. H. Frings, A. van der Liet, A. Menovsky, and A. de Visser, Physica B + C **123**, 11 (1983).
[14] L. Havela, A. V. Kolomiets, V. Sechovsky, P. Javorsky, T. D. Cuong, J. Kamarad, and N. Sato, Acta Phys. Slovaca **48**, 803 (1998).
[15] A. V. Kolomiets, L. Havela, V. Sechovsky, P. Javorsky, J. Kamarad, N. Sato, and T. D. Cuong, Physica B **259–261**, 238 (1999).
[16] A. Kolomiets, L. Havela, J. Prchal, and A. Andreev, J. Korean Phys. Soc. **62**, 1572 (2013).
[17] B. Bireckoven and J. Wittig, J. Phys. E: Sci. Instrum. **21**, 841 (1988).
[18] N. F. Mott, Philos. Mag. **26**, 1015 (1972).
[19] J. H. Mooij, Phys. Status Solidi A **17**, 521 (1973).
[20] J. S. Dugdale, Contemp. Phys. **28**, 547 (1987).
[21] Y. Imry, Phys. Rev. Lett. **44**, 469 (1980).
[22] B. S. Chandrasekhar and J. K. Hulm, J. Phys. Chem. Solids **7**, 259 (1958).
[23] R. A. Steeman, E. Frikkee, S. A. M. Mentlik, A. A. Menovsky, J. G. Nieuwenhuys, and J. A. Mydosh, J. Phys.: Condens. Matter **2**, 4059 (1990).
[24] M. Samsel-Czekala, E. Talik, R. Troc, and J. Stepien-Damm, Phys. Rev. B **77**, 155113 (2008).
[25] D. Wohlleben and B. Wittershagen, Adv. Phys. **34**, 403 (1985).
[26] Y. Tsiovkin, M. A. Korotin, A. O. Shorikov, V. I. Anisimov, A. N. Voloshinskii, A. V. Lukoyanov, E. S. Koneva, A. A. Povzner, and M. A. Surin, Phys. Rev. B **76**, 075119 (2007).
[27] J. A. Blanco, D. Gignoux, J. C. Gomez-Sal, J. Rodriguez Fernandez, and D. Schmitt, J. Magn. Magn. Mater. **104–107**, Part 2, 1285 (1992).
[28] J. A. Blanco, D. Gignoux, J. C. Gomez Sal, J. Rodriguez Fernandez, and D. Schmitt, Physica B **175**, 349 (1991).
[29] T.-H. Tsai and D. J. Sellmyer, Phys. Rev. B **20**, 4577 (1979).
[30] S. Doniach, Physica B + C **91**, 231 (1977).
[31] B. Coqblin and J. R. Schrieffer, Phys. Rev. **185**, 847 (1969).
[32] B. R. Cooper, R. Siemann, D. Yang, P. Thayamballi, and A. Banerjea, in *Handbook on the Physics and Chemistry of the Actinides*, edited by A. J. Freeman and G. H. Lander (North-Holland, Amsterdam, 1985), Vol. 2, p. 435.

[33] A. L. Cornelius, J. S. Schilling, O. Vogt, K. Mattenberger, and U. Benedict, J. Magn. Magn. Mater. **161**, 169 (1996).
[34] V. Sechovský, F. Honda, K. Prokeš, J. C. Griveau, A. V. Andreev, Z. Arnold, J. Kamarád, and G. Oomi, J. Magn. Magn. Mater. **290–291**, 629 (2005).
[35] Y. Haga, F. Honda, G. Oomi, T. Kagayama, N. Mori, T. Nakanishi, Y. Tokiwa, D. Aoki, and Y. Onuki, J. Phys. Soc. Jpn. **71**, 2019 (2002).
[36] L. Havela, V. Sechovsky, F. R. de Boer, E. Brück, and H. Nakotte, Physica B **177**, 159 (1992).
[37] Y. Kuroiwa, M. Kohgi, T. Osakabe, N. Sato, and Y. Onuki, JAERI-M (1993).
[38] E. Holland-Moritz and G. H. Lander, in *Handbook on the Physics and Chemistry of Rare Earths, Lanthanides/Actinides: Physics-II*, edited by K. A. Gschneidner, Jr., L. Eyring, G. H. Lander, and G. R. Choppin (Elsevier Science B.V., Amsterdam, 1994), Vol. 19, p. 1.
[39] R. D. Hoffmann and R. Pottgen, Z. Kristallogr. **216**, 127 (2001).
[40] F. R. de Boer *et al.*, Physica B **176**, 275 (1992).
[41] L. Havela, R. V. Dremov, A. V. Andreev, V. Sechovský, J. Šebek, and K. Prokeš, J. Alloys Compd. **271–273**, 418 (1998).
[42] L. Havela, T. Almeida, J. R. Naegele, V. Sechovsky, and E. Brück, J. Alloys Compd. **181**, 205 (1992).
[43] J.-S. Kang, S. C. Wi, J. H. Kim, K. A. McEwen, C. G. Olson, J. H. Shim, and B. I. Min, J. Phys.: Condens. Matter **16**, 3257 (2004).
[44] L. M. Sandratskii and J. Kubler, J. Phys.: Condens. Matter **9**, 4897 (1997).
[45] M. Kurisu, H. Kawanaka, T. Takabatake, and H. Fujii, J. Phys. Soc. Jpn. **60**, 3792 (1991).
[46] M. Nakashima *et al.*, J. Phys.: Condens. Matter **13**, L569 (2001).
[47] K. H. J. Buschow and H. J. Daal, *Comparison of Anomalies Observed in U- and Ce-Intermetallics*, edited by C. D. Graham, Jr. and J. J. Rhyne, AIP Conf. Proc. No. 5 (AIP, New York, 1972), p. 1464.
[48] V. Sechovsky and L. Havela, in *Handbook of Ferromagnetic Materials*, edited by E. P. Wohlfarth and K. H. J. Buschow (Elsevier, 1988), Vol. 4, p. 309.